Suppression of High-power Microwave Impact onto Diagnostic Detectors during ECR-heating of Fusion Plasmas

D. Zhang1, R. Burhenn1, M. Hirsch1, H.P. Laqua1, R. König1, J.W. Oosterbeek2, J. Baldzuhn1, P.A. Grodzki1, K. Ewert1, K. Grosser1, A. Cardella1 and the W7-X Team

1 Max-Planck-Institute für Plasmaphysik, EURATOM Ass., D-17491 Greifswald, Germany

2 Technische Universiteit Eindhoven, Den Dolech2, 5612 AZ Eindhoven, The Netherlands

1. Introduction

In fusion devices with powerfully ECR-heated plasmas non-absorbed microwave stray radiation exists unavoidably and is potentially harmful for any diagnostic components made of microwave-absorbing materials. For optical diagnostics, detectors are usually located in enclosures with apertures/windows opened to the plasma. Microwaves, also those beyond the optical viewing angles of the detectors, penetrate through the aperture/window into the cavity-like detector housing and impact the detectors through multi-reflection and diffraction. The impact can be due to thermal effects or electromagnetic disturbances. For bolometer diagnostics consisting of detectors having metal-foil absorbers, microwaves induce eddy currents in the foils, perturbing the measurements through thermal effect. Estimations and preliminary experiments performed on a prototype of the bolometer to be installed at W7-X indicated that the signal induced by the microwaves is comparable to that expected from the plasma radiation[1]. At W7-X the plasmas are heated by 140 GHz microwave radiation. The non-absorbed microwave stray radiation level[2] is 20-200 kW/m^2 which is so high that a metal-mesh screen with a transmission factor of 5% is even insufficient[1]. Developing suitable techniques to suppress the microwaves is thus essential to guarantee the functionality of this diagnostic. In this paper, common techniques for screening microwaves with metal-meshes are analyzed analytically. Optimization criteria are addressed to enhance the ratio of optical throughput to microwave power transmission. Screening the microwaves by a perforated metal plate is also analyzed. Antireflection coating on the inner surface of the detector housing for damping the stray radiation level in the detector housing is briefly described. This, together with a selected metal-mesh, is implemented in the bolometer prototype. Experimental results under high microwave power conditions are presented and explained.

2. Analytical analysis of microwave screens for optic detectors

Metal-mesh Metal-meshes or grids of round wires are commonly used for microwave screening. A basic condition for a microwave filter is that $g < \lambda/2$, where g is the wire spacing and λ the wavelength, respectively. According to the transmission line model, in the long-wavelength limit the field transmission coefficient t is determined by the equivalent impedance Z_g of the grid. In the lossless case it can be expressed as $t=1/(1+Z_{fs}/2Z_g)$, where $Z_{fs} = 120\pi\ \Omega$ for normal incidence in free space and Z_g depends on grid parameters and wavelength, i.e. $Z_g = -j\omega_0 \ln\left(\frac{g}{\pi d}\right) Z_{fs}/(\frac{\omega}{\omega_0} - \frac{\omega_0}{\omega})$, where d is the wire diameter ($d << \lambda$), $\omega=$

g/λ and $\omega_0 \approx 0.85$ defining the resonance location[3]. Fractional microwave power transmission T_m and shielding efficiency SE are obtained using $T_m = ABS(t^2)$ and $SE = 20\log(1/T_m)dB$,

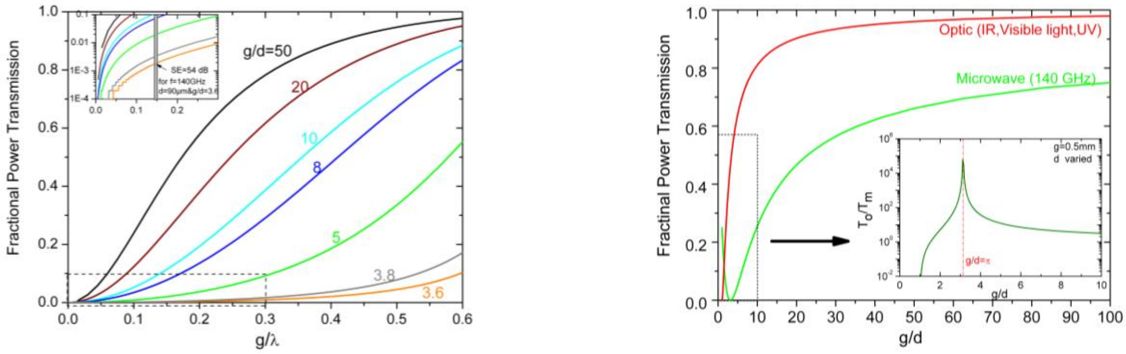

Fig. 1: (Left) Microwave transmissions as functions of grid parameters and wavelength for normal incidence and lossless wires. (Right) Transmissions for 140 GHz microwaves and for photons as function of g/d; their ratios are shown in the inset.

respectively. For various grid configurations T_m is shown in Fig. 1(left), which demonstrates that transmission increases as the spacing increases and as the wire size decreases. T_m also increases with the frequency and approaches unity asymptotically. Fig. 1(right) shows the 140 GHz microwave transmission T_m and the optic throughput T_o, based on $T_o=(1-d/g)^2$, as functions of grid parameter g/d. Keeping g as constant, increasing the wire thickness results in reducing transmission until $g/d = \pi$, where zero transmission or total reflection is reached. A maximum T_o/T_m ratio (show in the inset of Fig.1 right) is hence obtained. The corresponding T_o is 46%. This result provides a guideline for selecting wire-meshes with high SE. Meshes with $d = 90$ µm and $g/d = 3.6$ (close to π) show low transmissions with a SE of ~50 dB for 140 GHz (see the inset of Fig. 1, left) is selected for the experiments. Its optic throughput is $T_o = 53\%$.

It is noteworthy that thin wire-meshes can be used in an environment with a low heat flux from plasma radiation only. Otherwise, an edge heat sink or cooling is required, which is whereas less effective due to the low conductivities of the thin wires.

Perforated metal plate (PMT) PMTs with 2D-arranged equilateral array of circular holes are typically used as dichroic filters. The configurations, i.e., the spacing of the holes s, the hole diameter D and the plate thickness L, play together roles in shaping the transmission character of the filter. The holes acts as circular waveguides with a cutoff frequency of $f_c = c/1.706D$, where c is the speed of light. Dichroic filters function thus as high-pass filters. Properly designed PMTs with sufficiently high T_o can be used to shield optical detectors from microwave impacts. The transmission can be calculated based on the formula $T_m = 1/(1 - j[A + B\tanh(\beta L)]) - 1/(1 - j[A + B\coth(\beta L)\ ])$, where A, B, and β are functions of wavelength, hole spacing and size as well as the lattice structure [4]. The transmissions for circular openings having an equilateral triangular lattice structure are calculated keeping $s/D = 1.5$ fixed. The optical throughput, $T_o = \pi D^2/2\sqrt{3}\,s^2$, is then 40%. Fig. 2 shows the results for varied hole sizes and hole lengths L, respectively. The transmission decreases as the hole diameter decreases and as the plate thickness increases. Keeping $L = 1$ mm, SEs are obtained

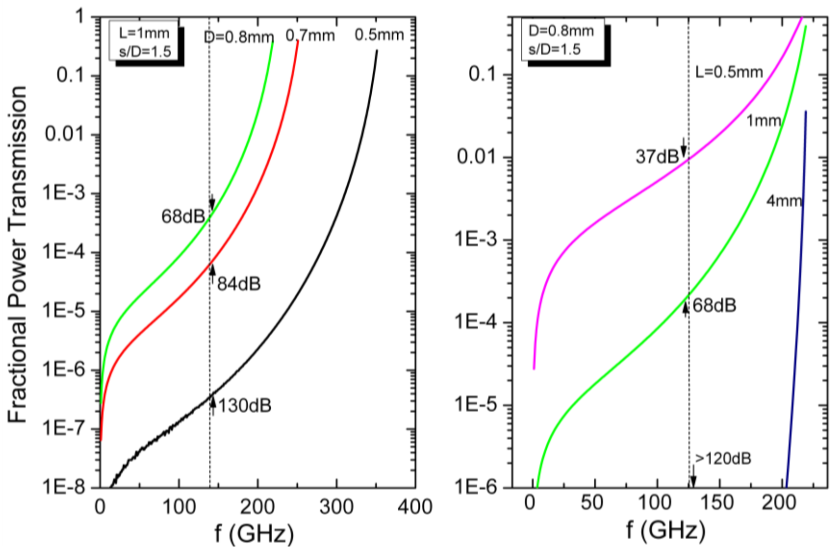

Fig. 2. Fractional microwave power transmissions for perforated metal plates with varied hole diameter (left) and plate thickness (right).

as 68 dB, 84 dB and 130 dB for 140 GHz microwave for D = 0.8 mm, 0.7 mm and 0.5 mm, respectively. The thickness L determines how strongly waves are attenuated in the evanescent region, thus controlling the sharpness of the cutoff characteristic (see Fig.2, right). Keeping D = 0.8 mm for L = 0.5 mm, 1.0 mm and 4.0 mm, SEs are 37 dB, 67 dB and >120 dB for 140 GHz microwave radiation, respectively.

3. Microwave trapping

Microwaves of power flux density P_m at the aperture enter the cavity-like detector housing and undergo multi-path reflections inside. Based on power balance the effective power flux density in the housing is expressed as $P_{m,eff} = P_m S_a/SUM(S_i \alpha_i)$, where S_a is the aperture area, S_i the surface of the elements forming the cavity and α_i the corresponding microwave absorption coefficient. Coating the inner surface with anti-reflecting materials, i.e. microwave absorber (e.g. Al_2O_3/TiO_2, B_4C), with α_i much larger than that of the common material (e.g. stainless steel, α_i = 2.6%) leads to a reduction of the $P_{m,eff}$. An alternative method is to use a set of properly spaced metal plates in the detector enclosure, being of lamella-like structure coated with anti-reflection layer, to prevent the microwaves to reach the bolometer absorber.

4. Experiment and results

A prototype of the W7-X bolometer has been tested in MISTRAL[5] which provides an isotropic, nearly homogenous microwave background with a power flux density of around 800 kW/m^2 for each single pulse. The detectors are gold-foil resistive type installed in a cylinder-shaped enclosure with a camera etendue, $E_t = S_a S_d / L_{ad}^2$ with S_a and S_d being the area of the aperture and the detector, and L_{ad} the distance between them, respectively, similar to that of the W7-X bolometer. A metal-mesh is selected as microwave screen and installed in the housing near to the detectors with a distance of 10mm to them and 7cm to the aperture. This arrangement reduces the heat flux onto the mesh, for the W7-X bolometer, by a factor of ~700, thus protects it from damage. The bronze-mesh with d = 90 µm and g/d = 3.6 having high SE (see Fig.1) and a desired T_o of 53% is used. The inner surface of the SS cylinder was

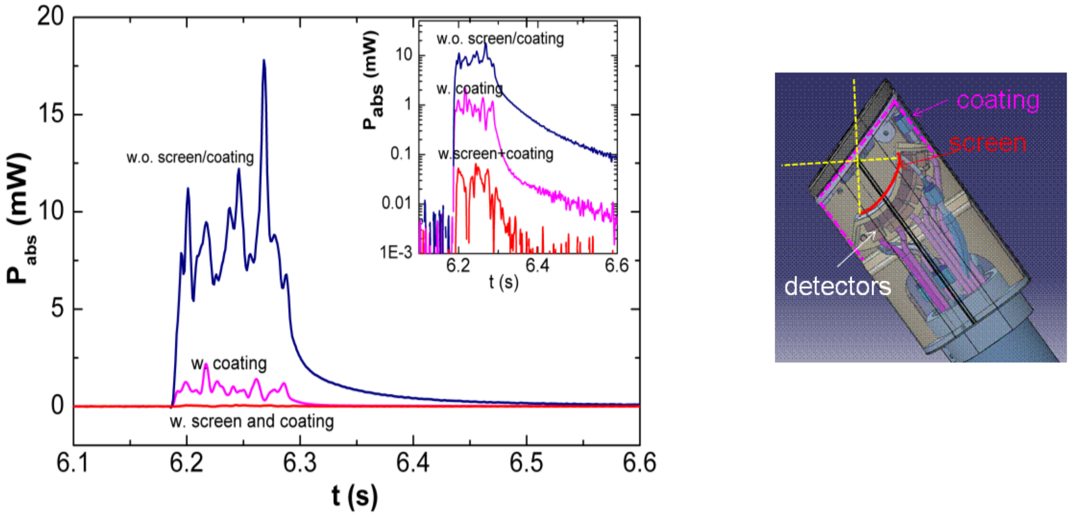

Fig.3. (Left) Comparison of bolometer signals with a prototype of W7-X bolometer tested in MISTRAL in the cases without and with microwave suppression. (Right) The bolometer camera designed for W7-X.

coated with a 150µm-Al_2O_3/TiO_2 layer (α_i =75%)[6]. Detector signals measured for cases without/with screen/coating are shown in Fig.3. The absorber coating leads to a reduction of the microwave impact by a factor of 10, being consistent with the estimated one based on the formula in section 3. The mesh screen suppresses the impact level by a further factor of 30 (i.e.30 dB, smaller that the calculated one, 50 dB, for an ideal mesh with perfect joints and lossless wires). Therefore, the microwave impact is attenuated by δ ~ 1/300 in total. The ratio of the microwave-induced signal to the plasma-radiation-induced one can be then estimated using $\eta = 2\pi\delta P_{m,eff}\alpha_{dm}S_d/P_{rad}\cdot E_t\cdot T_o\cdot\alpha_{dp}$ with $P_{rad,}$ denoting the power flux density of the plasma radiation at the entrance of the aperture, α_{dp} ~ 1 and α_{dm} ~ 0.1% being the absorption coefficients of the gold-foil detector to the radiations, respectively. Estimation for a typical case, P_{rad} = 50 kW/m^2 and P_m = 20 kW/m^2 yields η = 0.2%, indicating that the microwave impact is suppressed to a negligible level. It is to note that a stainless steel mesh with similar grid parameters provides a similar shielding efficiency as the bronze-mesh, but has a lower thermal conductivity.

The technique described above is adopted for the construction of the W7-X bolometer (see Fig. 3 (right). The concept, however, can be extended to designs of other (optical) diagnostics.

Reference

[1]. D. Zhang et al., Rev. Sci. Instrum. **81,** 10, 134 (2010)

[2]. H.P. Laqua *et al* 2001 *Proc. 28th EPS Conf. on Contr. Fusion and Plasma Phys.*, *Madeira*, **25A**, 1277-1280, P3.099

[3]. P.F. Goldsmith, *Quasioptical Systems: Gaussian Beam, Quasioptical. Propagation and Applications*. New York, IEEE Press, 1998.

[4]. C.C. Chen, IEEE Trans. Microwave Theory Tech. 21, 1-7, (**1973**).

[5]. S. Ullrich, H.J. Hartfuss, M. Hirsch, H. Laqua, *Stellarator News* 98, 2005.

[6]. Miriam Floristán et al., Fusion Engineering and Design (2010).